Nkx3.1 Controls the DNA Repair Response in the Mouse Prostate

Hailan Zhang,[1] Tian Zheng,[1,2] Chee Wai Chua,[1,3] Michael Shen,[1,3] and Edward P. Gelmann[1]*

[1]Department of Medicine and Pathology, Columbia University Medical Center, Herbert Irving Comprehensive Cancer Center, Columbia University, New York City, New York
[2]Department of Statistics, Columbia University Medical Center, Herbert Irving Comprehensive Cancer Center, Columbia University, New York City, New York
[3]Department of Developmental and Cell Biology, Columbia University Medical Center, Herbert Irving Comprehensive Cancer Center, Columbia University, New York City, New York

BACKGROUND. The human prostate tumor suppressor NKX3.1 mediates the DNA repair response and interacts with the androgen receptor to assure faithful completion of transcription thereby protecting against *TMPRSS2-ERG* gene fusion. To determine directly the effect of Nkx3.1 in vivo we studied the DNA repair response in prostates of mice with targeted deletion of *Nkx3.1*.
METHODS. Using both drug-induced DNA damage and γ-irradiation, we assayed expression of γ-histone 2AX at time points up to 24 hr after induction of DNA damage.
RESULTS. We demonstrated that expression of Nkx3.1 influenced both the timing and magnitude of the DNA damage response in the prostate.
CONCLUSIONS. Nkx3.1 affects the DNA damage response in the murine prostate and is haploinsufficient for this phenotype. *Prostate 76:402–408, 2016.*

KEY WORDS: **NKX3.1; DNA repair; haploinsufficiency; γhistone 2AX**

INTRODUCTION

Cancer arises in the prostate glands of the majority of aging males and is universally found at autopsy, often in multiple foci [1]. Less frequently one of the foci may undergo sufficient malignant progression to develop clinically significant invasive cancer with the capacity to metastasize [2]. Prostate mutagenesis occurs during the natural course of aging and can result from the action of the androgen receptor as well as from inflammatory changes that are presumed to generate reactive oxygen species that react with DNA [3–6]. The prostate specific homeodomain protein NKX3.1 is a key element in protecting prostate epithelial cells from DNA damage [7]. NKX3.1 complexes with androgen receptor to mediate DNA repair of potentially mutagenic lesions generated during transcriptional activation [8]. NKX3.1 also is activated by DNA damage and accelerates the DNA damage repair response by activating ATM [9].

Although the interaction of NKX3.1 with the DNA damage response has been demonstrated biochemically and in cultured cells, the effect on the DNA damage response in vivo has not been proven. We

Grant sponsor: NCI; Grant number: P01 CA154293; Grant sponsor: CCSG; Grant number: P30 CA013696-36.

The authors have no competing interests and no conflicts to disclose.

*Correspondence to: Dr. Edward P. Gelmann, Department of Medicine and Pathology, Columbia University Medical Center, Herbert Irving Comprehensive Cancer Center, Columbia University, 177 Ft. Washington Ave., MHB 6N/435, New York, NY 10032. E-mail: gelmanne@columbia.edu
Received 21 September 2015; Accepted 20 November 2015
DOI 10.1002/pros.23131
Published online 10 December 2015 in Wiley Online Library (wileyonlinelibrary.com).

subjected *Nkx3.1* gene targeted mice to DNA damage insults in order to examine the effect of Nkx3.1 on the DNA damage response as indicated by the appearance of γ-histone2AX (γH2AX) in prostate epithelial cells. We show here that expression of Nkx3.1 affects both the magnitude and the timing of the DNA damage response in the mouse prostate.

MATERIALS AND METHODS

Antibodies

Mouse anti-phospho-histone H2A.X (Ser 139; # 05-636) was purchase from Millipore (Temecula, CA) and a 1:500 dilution was used for immunofluorescent staining. Rabbit anti-cytokeratin 8 (CK8; # EP16284) was purchased from Abcam (Cambridge, MA) and a 1:300 dilution was used for immunofluorescent staining.

The CK5 antibody was originally from Covance (Princeton, NJ; Cat. # SIG-3475) but now is sold by BioLegend (San Diego, CA; Cat. # 905901). 1:1000 dilution was used. Fluorescent secondary antibodies including Alexa Fluor 488 F(ab′) 2 fragment of goat anti-rabbit IgG (H+L; #A11070) and Alexa Fluor 568 F(ab′) 2 fragment of goat anti-mouse IgG (H+L; #A11019) were purchase from Life Technologies (Eugene, OR). A 1:500 dilution was for immunofluorescent staining.

Animals

Wild-type C57 BL/6 mice were purchased from Taconic Biosciences (Hudson, NY) and bred in the animal facility at Columbia University Medical Center. The *Nkx3.1* homozygous mutant ($Nkx3.1^{-/-}$) mice on the C57 BL/6 background were initially provided by Dr. Michael Shen and then bred in the animal facility. The *Nkx3.1* heterozygous mutant ($Nkx3.1^{+/-}$) mice were generated by mating the C57 BL/6 mice with the $Nkx3.1^{-/-}$ mice. All mouse work was performed in accordance with the policies and regulations of the Institutional Animal Care and Use Committee of Columbia University.

Induction of DNA Damage Response in Mice

Etoposide (# E1383) and mitomycin C (# M4287) were purchased from Sigma–Aldrich (St. Louis, MO). Etoposide was dissolved in dimethyl sulfoxide (DMSO; 50 mg/ml) for storage at −20EC and was diluted before injection to 0.5 mg/ml in phosphate buffered saline (PBS) at room temperature. Mitomycin C was dissolved in PBS at 20 mg/ml for storage at −20EC and diluted to 0.2 mg/ml in PBS before injection. Male wild type, $Nkx3.1^{+/-}$, and/or $Nkx3.1^{-/-}$ mice of 8–12 weeks old were given single doses of either etoposide (6 mg/kg) or mitomycin C (3 mg/kg) by intraperitoneal injection. The sham-treated mice were injected with the same volume of PBS. Mice were sacrificed at various times to assay organs for expression of γH2AX. Mouse prostate lobes and other tissues were dissected and subject to fixation in 4% formaldehyde in PBS. Processed tissues were embedded in paraffin and sectioned at 0.5 μm. To induce DNA damage by γ-irradiation mice of 8–12 weeks old were given a single dose of 15 Gy using a Gammacell 40 Exactor (Best Theratronics, Ottawa, Canada). Tissues were dissected, fixed, processed, and sectioned as described above.

Measurement of Etoposide Levels in Mouse Tissues

Mice 8–12 weeks old were given a single dose of etoposide (6 mg/kg) by intraperitoneal injection. Tissues (prostate gland, seminal vesicle, liver and intestine) were collected 2–8 hr after etoposide injection and flash frozen with liquid nitrogen. Frozen samples were homogenized in water and then extracted with 5 ml of methyl tert-butyl ether. The supernatant was then evaporated under nitrogen and the solute resuspended in 100 μl 75% methanol. Separation was performed using an Agilent 1290 UHPLC system with a 50 mm Poroshell 120EC-C18 column equilibrated with 90% water with 0.1% formic acid and 10% methanol with 0.1% formic acid. An Agilent 6410 Triple Quadrupole Mass Spectrometer was used for analyte detection.

Immunofluorescence Analysis

Tissue sections were deparaffinized and rehydrated by subsequent treatment with xylenes, 100%, 95%, 75%, and 50% ethanol and water. After steaming in 0.01 M sodium citrate, pH 6.0, for 15 min for antigen retrieval, sections were treated with 0.5% Triton X-100 in PBS for 10 min followed by blocking in 10% goat serum in PBS 0.1% Triton X-100 (PBST) for 1 hr at room temperature. After washing in PBS for 5 min, sections were incubated for 5 min with 3% goat serum in PBST followed by incubation with primary antibodies in 3% goat serum in PBST at 4EC overnight or at room temperature for 2 hr. After washing in PBST, sections were incubated with fluorescent secondary antibodies at room temperature in the dark for 1 hr. Sections were then washed with PBST and mounted using Vectashield Antifade Mounting Medium with DAPI (Vector Laboratories, Burlingame, CA). Sections were viewed and photographed using a Leica TCS SP3

confocal microscope (Leica Microsystems, Buffalo Grove, IL). For quantitative studies, fluorescence and DAPI labeled cell nuclei were counted using the Image J software developed by Wayne Rasband at the NIH. For the gamma H2AX staining in prostate sections of irradiated mice, the ImageJ program was used to quantitate intensity of gamma H2AX staining. Each image was split into three channels (blue, green, and red). The areas of DAPI stained nuclei (blue) were selected by tracing and the integrated density of the DAPI staining of each nucleus was measured. The selected areas were then applied to the same nuclei in the red channel and intensity of the γH2AX staining was measured for each nucleus. For each section 500 nuclei were measured and the average intensity was used to calculate the ratio of the γH2AX staining intensity to the DAPI staining intensity. For drug-treated mice ImageJ was used to detect DAPI and γH2AX positive nuclei, respectively, and the ratio of γH2AX-positive nuclei to DAPI-positive nuclei was then determined.

Statistical Analysis

The effect of time on γH2AX expression did not exhibit a linear trend, we, therefore, fitted nonlinear regression models that set time as a categorical variable. We assumed the effect of time on the measurements can take any form. The analysis of variance (ANOVA) method was used to compare between-group differences between two regression models. The null model assumed no difference between the groups, whereas the alternative model assumed the genotype groups are different. The ANOVA method tested the fit of the null model (the black broken line) fitted to all genotype groups pooled together (assuming that they have the same trend) against the alternative model that the different genotype groups are assumed to have different model (the colored lines). The small *P*-value suggested that there were statistically significant differences between the temporal trends in the two groups. To verify the significant test results were not due to outliers presented in the measured values or sensitive to the distribution of measurement values, we converted all measurement values to rank values and repeat the analysis. We obtained identical conclusions as in the analyses using original numerical values.

RESULTS

γ-Irradiation

Mice were subjected to γ-irradiation with 15 Gy using a shielding device to expose the pelvic region. Results of immunohistochemical staining for γH2AX in anterior prostate are shown in Figure 1A. Staining varied in intensity based on the presence of two copies of *Nkx3.1*. Importantly, the robust and early DNA damage response was seen predominantly in luminal epithelial cells as indicated by staining with cytokeratin 8 as compared to cytokeratin 5 (Supplementary Fig. S1). This evidence of a more robust DNA damage response at 1.5 hr after irradiation is in contrast to the more robust γH2AX staining seen preferentially in basal cells 8–24 hr after induction of DNA damage [10]. Intact mice showed a statistically different result from *Nkx3*.1 deletion mice, but heterozygous mice did not (Supplementary Fig. S2A and B). An example of the histologic sections from the 1.5 hr time point is shown in Figure 2. In contrast to differences in prostate γH2AX staining based on *Nkx3.1* genotype, seminal vesicle and small intestine showed staining that varied with time, but not with genotype (Figs. 2 and 3). The magnitude of the DNA repair response to γ-irradiation varied depending on *Nkx3.1* copy number, but not the timing. We also tested the DNA repair response to etoposide and to mitomycin C.

Etoposide

Etoposide binds to topoisomerase II, arrests it on DNA after DNA cleavage, and causes single and double-strand DNA breaks [11,12]. Mice were treated once with etoposide intraperitoneally and tissues were analyzed for γH2AX staining after exposure. To ascertain uptake of the drug we assayed etoposide levels in prostatic lobes, seminal vesicle, liver, and small intestine 30 min after administration of etoposide intraperitoneally. As expected the highest concentration of drug was in the liver that is the first organ to be exposed to an agent administered intraperitoneally (Supplementary Table SI). However, all tissues were seen to have substantial levels of etoposide. The DNA damage response after etoposide administration was rapid in intact mice, but delayed 6 hr in *Nkx3.1*$^{-/-}$ mice (Fig. 1B). Importantly, in *Nkx3.1*$^{+/-}$ mice that are known to develop a dysplastic phenotype later in life, the DNA damage response had similar timing to the intact mouse, but was markedly attenuated similar to the attenuation seen for the response to γ-irradiation. The results for intact mice were statistically different from both heterozygous and knock out mice (Supplementary Fig. S2C and D).

Mitomycin C

Mitomycin C produces interstrand DNA crosslinks and secondary double-strand breaks [10,11]. Repair of

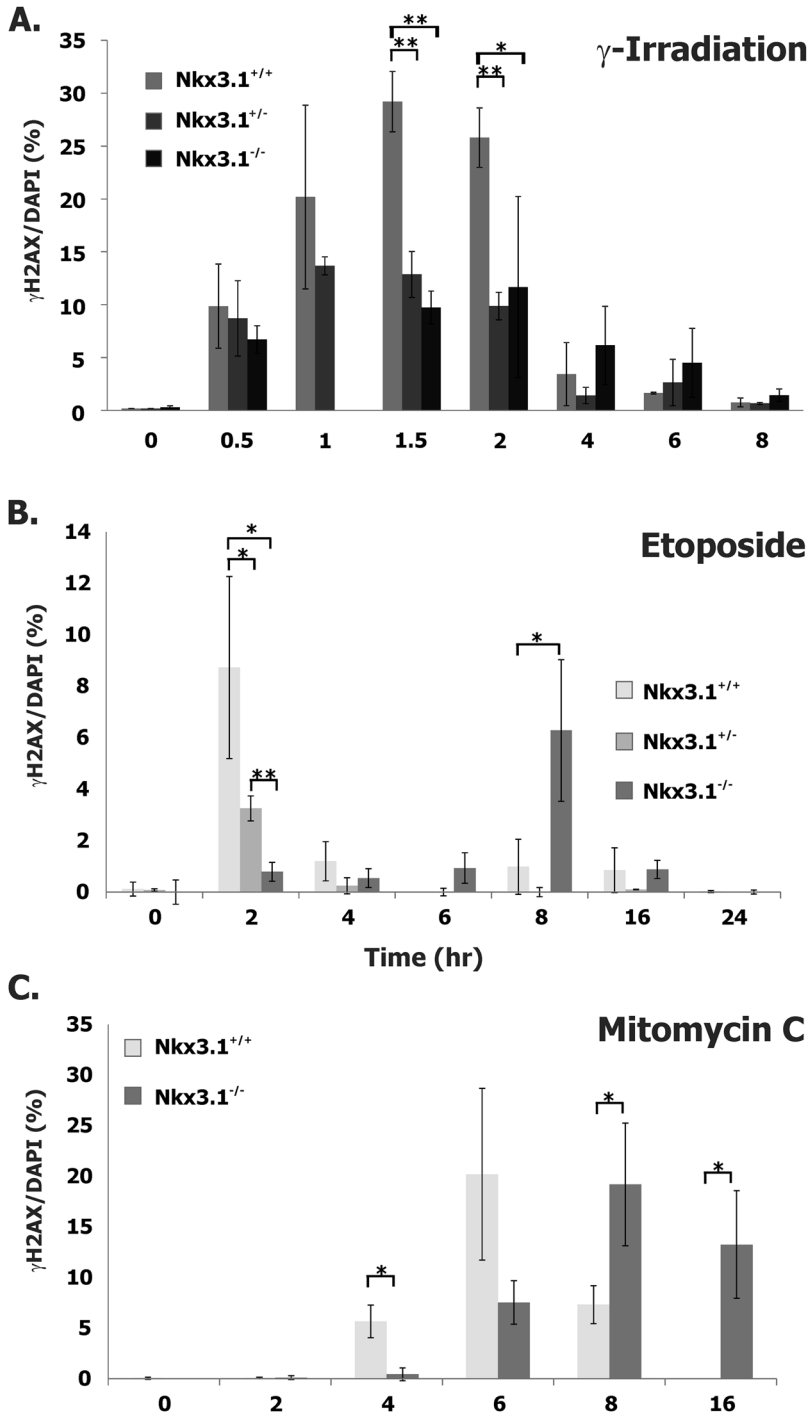

Fig. 1. γH2AX expression in murine prostates after DNA damage. **A**: Fifteen gray pelvic irradiation. **B**: Etoposide 6 mg/kg intraperitoneally. **C**: Mitomycin C 3 mg/kg intraperitoneally. Absence of data for heterozygous mice in A and C was due to limitations in supply of these animals. $^{*}P < 0.05$ and $^{**}P < 0.005$.

DNA crosslink damage has to involve both strands of DNA and may utilize more than one DNA repair pathway including nucleotide excision repair (NER) and homology-directed DNA repair [12,13]. The DNA damage response to 3 mg/kg intraperitoneal mitomycin C in intact mice showed a peak of γH2AX staining at 6 hr and in Nkx3.1$^{-/-}$ mice γH2AX was seen most pronounced at 8 hr after exposure (Fig. 1C). Heterozygous mice were not tested with mitomycin C due to animal supply. Differences between the two genotypes were highly statistically significant (Supplementary Fig. S2E and F).

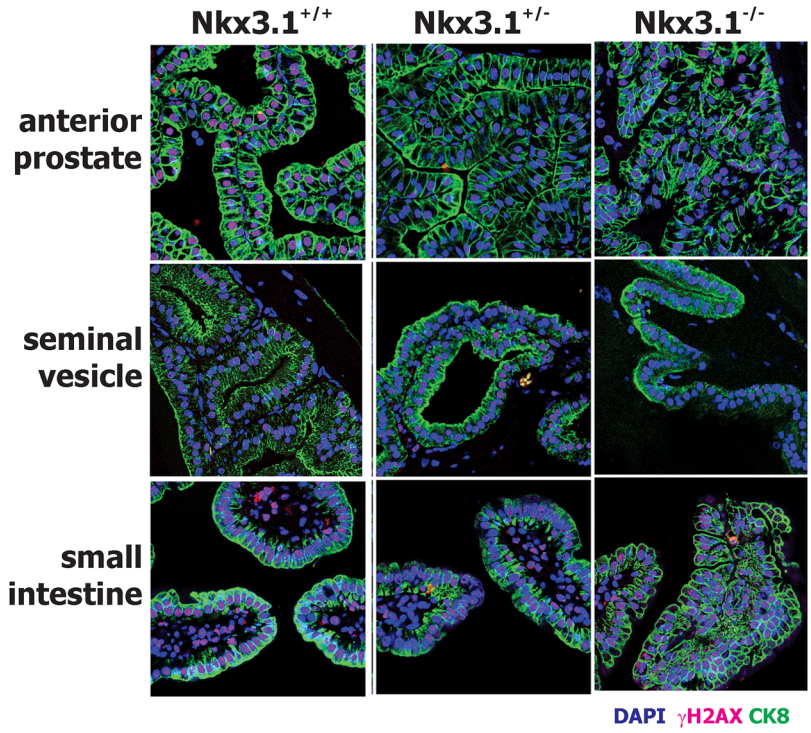

Fig. 2. Micrographs from immunofluorescence microscopy from *Nkx3.1* gene-targeted mice 1.5 hr after 15 Gy exposure. Staining was performed for γH2AX and cytokeratin 8. Counterstain for nuclei was done with DAPI.

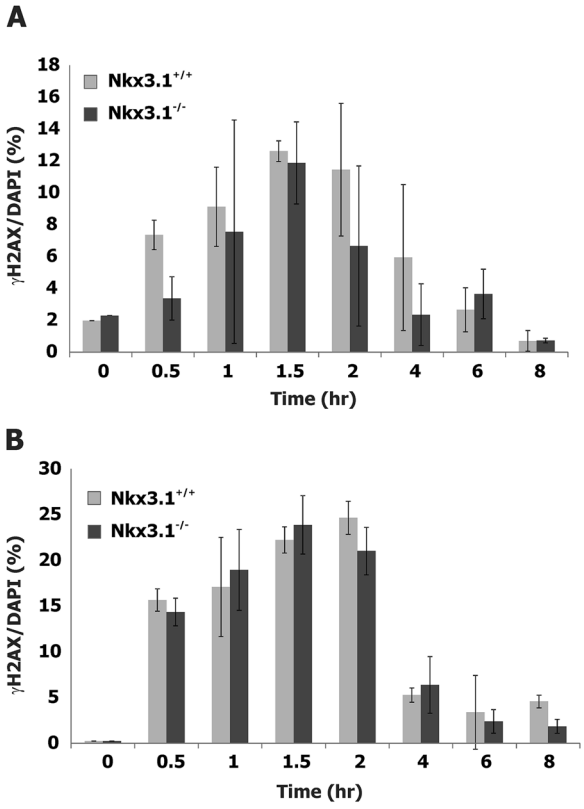

Fig. 3. γH2AX staining of **A**. seminal vesicle and **B**. small intestine from mice after 15 Gy exposure.

DISCUSSION

The prostate gland is susceptible to a greater degree of oncogenesis than most organs. This may be due to an ongoing exposure to inflammation and oxidative stress than is present in most tissues. Also, prostate mutagenesis results from physiologic activity of a key prostate epithelial cell survival factor, androgen. Androgen action is required to sustain the integrity of the prostate and prostate epithelial cells are constantly responding to androgenic hormones [13]. Steroid hormone receptors bind to DNA to activate transcription via a mechanism that includes the formation of 8-oxoguanine adducts, the most common DNA modification that results from oxidative DNA damage as well [14]. Androgen receptor is the key initiator of the most common chromosomal translocation in prostate cancer, that of fusion of the *TMPRSS2* promoter and *ERG* gene that are syntenic on chromosome 21 [3]. In fact, this single gene fusion event that is found in more than half of human prostate cancer is completely dependent on the presence of androgen and activation of its receptor [15]. Thus, it follows that mechanistic adaptations evolved to assure accurate and rapid DNA repair in cells constantly exposed to mitogenic stimuli like prostate epithelial cells. Nkx3.1 regulates the magnitude and timing of the acute response to DNA damage in prostate luminal epithelial cells. Based on

our prior findings, the effect of NKX3.1 on the DNA damage response is important for cellular integrity and for prevention of pathogenic DNA lesions such as TMPRSS2-ERG rearrangement [7,16]. It is noteworthy that basal epithelial cells do not express NKX3.1 or apparently require an accelerated response to DNA repair. Strikingly, *Nkx3.1* deletion in murine luminal epithelial cells results in maximal expression of γH2AX at 8 hr after DNA damage, consistent with the observation that in that time frame after DNA damage basal epithelial cells express more γH2AX than do luminal cells [10].

In human prostate cells, NKX3.1 binds at the DNA site of AR binding and transcriptional activation and mediates proper DNA repair, protecting against *TMPRSS2-ERG* fusion [17]. NKX3.1 acts by forming a complex with androgen receptor and by recruiting key enzymes essential for DNA repair. For example, NKX3.1 binds to topoisomerase I and markedly activates its DNA resolving activity [18]. Topoisomerase I is both a key component recruited to the AR transcriptional complex and important for access of DNA repair proteins to sites of DNA damage [8]. NKX3.1 also binds to ATM and recruits it to sites of DNA damage [7,19]. Moreover, NKX3.1 itself undergoes tyrosine phosphorylation within minutes of DNA damage in order to trigger its interaction with ATM [9].

The prostate also undergoes histologic changes during aging including atrophic regions of inflammation [6]. It is in these regions where inflammatory cells increase the formation of reactive oxygen species that cytokines are generated as well. Loss of NKX3.1 precisely in regions of inflammatory atrophy is mediated by inflammatory cytokines and thereby results in enhanced vulnerability to mutagenesis [20–22]. Thus, the physiologic aging process is accompanied by changes that increase the likelihood of mutagenesis due to regional reductions in NKX3.1 at sites of inflammation. It is also noteworthy that prostatitis is a risk factor for the later development of prostate cancer [23].

NKX3.1 loss results from both genetic and epigenetic events that occur in preinvasive prostate cancer [24]. Genetic loss is caused by monoallelic deletion of 8p21, the most common single genetic event in prostate carcinogenesis [25,26]. The mechanism underlying preferential loss of 8p21 is not understood, but clearly *NKX3.1* is the target of this common genetic event [27]. Moreover, the degree of NKX3.1 protein loss in primary prostate cancer varies from levels as low as 30% of normal cell levels to 90% of normal cell levels. The degree of NKX3.1 protein loss correlates with the propensity for *TMRPSS2-ERG* rearrangement, reflecting attenuated DNA repair [17]. Also, lower levels of NKX3.1 correlated with higher Gleason grade and therefore diminished long-term prognosis [16,24].

The demonstration that *Nkx3.1* loss or even heterozygosity affects the DNA damage response is further evidence that the multifunctional homeodomain protein was adapted to address the critical physiologic susceptibility of the prostate gland to DNA damage. The DNA damage response after γ-irradiation was affected in magnitude by Nkx3.1 levels, but not in timing. In contrast, the two chemical agents administered intraperitoneally induced DNA damage for which the responses were delayed in the absence of Nkx3.1, but not reduced in magnitude. *Nkx3.1* heterozygosity did not result in a response delay in etoposide-treated mice, but did attenuate the DNA damage response. These results are consistent with the premise that Nkx3.1 plays a regulatory role for the activation of ATM and other DNA damage response proteins. That role may vary with the type of DNA damage and the timing of exposure as irradiation is instantaneous, but intraperitoneal administration of drugs may results in more prolonged exposure to DNA damage insults.

We can now speculate about the evolutionary drive that underlies the role of Nkx3.1 in DNA repair. As the mouse is not subject either to effects of aging on the prostate or to dietary insults that increase prostate cancer risk in humans, the evolutionary adaptation of Nkx3.1 may have been to address DNA damage caused by AR action in prostate epithelium. Loss of NKX3.1 thus may be the key molecular mechanism underlying age-related prostate carcinogenesis in man.

CONCLUSIONS

Nkx3.1 regulates the timing and magnitude of the DNA damage response in the murine prostate. Similar to its effects on prostate neoplasia, Nkx3.1 is haploinsufficient with regard to its role in the DNA damage response.

REFERENCES

1. Bostwick DG, Shan A, Qian J, Darson M, Maihle NJ, Jenkins RB, Cheng L. Independent origin of multiple foci of prostatic intraepithelial neoplasia: Comparison with matched foci of prostate carcinoma. Cancer 1998;83(9):1995–2002.
2. Effert P, Neubauer A, Walther PJ, Liu ET. Alterations of the p53 gene are associated with the progression of a human prostate carcinoma. J Urol 1992;147:789–793.
3. Mani RS, Tomlins SA, Callahan K, Ghosh A, Nyati MK, Varambally S, Palanisamy N, Chinnaiyan AM. Induced chromosomal proximity and gene fusions in prostate cancer. Science 2009;326(5957):1230.

4. Haffner MC, Aryee MJ, Toubaji A, Esopi DM, Albadine R, Gurel B, Isaacs WB, Bova GS, Liu W, Xu J, Meeker AK, Netto G, De Marzo AM, Nelson WG, Yegnasubramanian S. Androgen-induced TOP2B-mediated double-strand breaks and prostate cancer gene rearrangements. Nat Genet 2010;42(8):668–675.
5. Weischenfeldt J, Simon R, Feuerbach L, Schlangen K, Weichenhan D, Minner S, Wuttig D, Warnatz HJ, Stehr H, Rausch T, Jager N, Gu L, Bogatyrova O, Stutz AM, Claus R, Eils J, Eils R, Gerhauser C, Huang PH, Hutter B, Kabbe R, Lawerenz C, Radomski S, Bartholomae CC, Falth M, Gade S, Schmidt M, Amschler N, Hass T, Galal R, Gjoni J, Kuner R, Baer C, Masser S, von KC, Zichner T, Benes V, Raeder B, Mader M, Amstislavskiy V, Avci M, Lehrach H, Parkhomchuk D, Sultan M, Burkhardt L, Graefen M, Huland H, Kluth M, Krohn A, Sirma H, Stumm L, Steurer S, Grupp K, Sultmann H, Sauter G, Plass C, Brors B, Yaspo ML, Korbel JO, Schlomm T. Integrative genomic analyses reveal an androgen-driven somatic alteration landscape in early-onset prostate cancer. Cancer Cell 2013;23(2):159–170.
6. Nelson WG, De Marzo AM, Isaacs WB. Prostate cancer. N Engl J Med 2003;349(4):366–381.
7. Bowen C, Gelmann EP. NKX3.1 activates cellular response to DNA damage. Cancer Res 2010;70(8):3089–3097.
8. Puc J, Kozbial P, Li W, Tan Y, Liu Z, Suter T, Ohgi KA, Zhang J, Aggarwal AK, Rosenfeld MG. Ligand-dependent enhancer activation regulated by topoisomerase-I activity. Cell 2015;160(3):367–380.
9. Bowen C, Ju JH, Lee JH, Paull TT, Gelmann EP. Functional activation of ATM by the prostate cancer suppressor NKX3.1. Cell Rep 2013;4(3):516–529.
10. Jaamaa S, Af Hallstrom TM, Sankila A, Rantanen V, Koistinen H, Stenman UH, Zhang Z, Yang Z, De Marzo AM, Taari K, Ruutu M, Andersson LC, Laiho M. DNA damage recognition via activated ATM and p53 pathway in nonproliferating human prostate tissue. Cancer Res 2010;70(21):8630–8641.
11. Long BH, Musial ST, Brattain MG. Single- and double-strand DNA breakage and repair in human lung adenocarcinoma cells exposed to etoposide and teniposide. Cancer Res 1985; 45(7):3106–3112.
12. Tewey KM, Chen GL, Nelson EM, Liu LF. Intercalative antitumor drugs interfere with the breakage-reunion reaction of mammalian DNA topoisomerase II. J Biol Chem 1984; 259(14):9182–9187.
13. Isaacs JT. Antagonistic effect of androgen on prostatic cell death. Prostate 1984;5:545–545.
14. Perillo B, Ombra MN, Bertoni A, Cuozzo C, Sacchetti S, Sasso A, Chiariotti L, Malorni A, Abbondanza C, Avvedimento EV. DNA oxidation as triggered by H3K9me2 demethylation drives estrogen-induced gene expression. Science 2008;319(5860):202–206.
15. Tomlins SA, Laxman B, Varambally S, Cao X, Yu J, Helgeson BE, Cao Q, Prensner JR, Rubin MA, Shah RB, Mehra R, Chinnaiyan AM. Role of the TMPRSS2-ERG gene fusion in prostate cancer. Neoplasia 2008;10(2):177–188.
16. Bowen C, Zheng T, Gelmann EP. NKX3.1 suppresses TMPRSS2-ERG gene rearrangement and mediates repair of androgen receptor-induced DNA damage. Cancer Res 2015.
17. Bowen C, Zheng T, Gelmann EP. NKX3.1 suppresses TMPRSS2-ERG gene rearrangement and mediates repair of androgen receptor-induced DNA damage. Cancer Res 2015;75(13):2686–2698.
18. Bowen C, Stuart A, Ju JH, Tuan J, Blonder J, Conrads TP, Veenstra TD, Gelmann EP. NKX3.1 homeodomain protein binds to topoisomerase I and enhances its activity. Cancer Res 2007;67(2):455–464.
19. Erbaykent-Tepedelen B, Karamil S, Gonen-Korkmaz C, Korkmaz KS. DNA damage response (DDR) via NKX3.1 expression in prostate cells. J Steroid Biochem Mol Biol 2014;141:26–36.
20. Bethel CR, Faith D, Li X, Guan B, Hicks JL, Lan F, Jenkins RB, Bieberich CJ, De Marzo AM. Decreased NKX3. 1 protein expression in focal prostatic atrophy, prostatic intraepithelial neoplasia, and adenocarcinoma: Association with gleason score and chromosome 8p deletion. Cancer Res 2006;66(22):10683–10690.
21. Khalili M, Mutton LN, Gurel B, Hicks JL, De Marzo AM, Bieberich CJ. Loss of Nkx3.1 expression in bacterial prostatitis: A potential link between inflammation and neoplasia. Am J Pathol 2010;176(5):2259–2268.
22. Markowski MC, Bowen C, Gelmann EP. Inflammatory cytokines induce phosphorylation and ubiquitination of prostate suppressor protein NKX3.1. Cancer Res 2008; 68(17):6896–6901.
23. Roberts RO, Bergstralh EJ, Bass SE, Lieber MM, Jacobsen SJ. Prostatitis as a risk factor for prostate cancer. Epidemiology 2004;15(1):93–99.
24. Asatiani E, Huang WX, Wang A, Rodriguez OE, Cavalli LR, Haddad BR, Gelmann EP. Deletion, methylation, and expression of the NKX3.1 suppressor gene in primary human prostate cancer. Cancer Res 2005;65(4):1164–1173.
25. Lapointe J, Li C, Giacomini CP, Salari K, Huang S, Wang P, Ferrari M, Hernandez-Boussard T, Brooks JD, Pollack JR. Genomic profiling reveals alternative genetic pathways of prostate tumorigenesis. Cancer Res 2007;67(18):8504–8510.
26. Taylor BS, Schultz N, Hieronymus H, Gopalan A, Xiao Y, Carver BS, Arora VK, Kaushik P, Cerami E, Reva B, Antipin Y, Mitsiades N, Landers T, Dolgalev I, Major JE, Wilson M, Socci ND, Lash AE, Heguy A, Eastham JA, Scher HI, Reuter VE, Scardino PT, Sander C, Sawyers CL, Gerald WL. Integrative genomic profiling of human prostate cancer. Cancer Cell 2010;18(1):11–22.
27. Swalwell JI, Vocke CD, Yang Y, Walker JR, Grouse L, Myers SH, Gillespie JW, Bostwick DG, Duray PH, Linehan WM, Emmert-Buck MR. Determination of a minimal deletion interval on chromosome band 8p21 in sporadic prostate cancer. Genes Chromosomes Cancer 2002;33(2):201–205.

SUPPORTING INFORMATION

Additional supporting information may be found in the online version of this article at the publisher's web-site.